A systematic DFT study of substrate reconstruction effects due to thiolate and selenolate adsorption

Katrin Forster-Tonigold[a] and Axel Groß[a,b]
[a] *Helmholtz Institute Ulm, D-89069 Ulm, Germany*
[b] *Institute of Theoretical Chemistry, Ulm University, D-89069 Ulm, Germany*

Possible adsorbate induced reconstruction effects of methanethiolate (MeS) and methaneselenolate (MeSe) on Au(111) are studied employing density functional theory (DFT). For the purposes of this study these simple alkanechalcogenates prove to be representative models for chalcogenate molecules with larger rest groups. MeS and MeSe show very similar properties regarding the adsorption at the unreconstructed and reconstructed surfaces. The latter are constructed by systematically introducing defects at various adsorbate coverages. It turns out that only if the defect site is occupied by at least two molecules the costs of creating the defect can be counterbalanced by the energetic gain and thus adsorbate induced reconstruction gets energetically feasible. Furthermore, for various molecular coverages the adatom-dichalcogenate model, as found by Maksymovych et al. (Phys. Rev. Lett. **97** (2006) 146103), is indeed the most stable reconstruction motif among the simple models studied herein. In order to mimic the impact of the environment, e.g. solvent effects, temperature or electric potentials, the stability of the reconstruction motifs were studied as a function of both the chemical potential of the adsorbate and the energy needed to create the defect substrate structure following the ansatz of ab initio atomistic thermodynamics. This approach hints at the fact that different reconstruction motifs can be realized in different chemical environments.

Keywords: thiolates, metal surfaces, adsorption, density functional theory calculations, correction for dispersion

I. INTRODUCTION

There is a long-standing interest in the preparation of self-assembled monolayers (SAMs) on substrates as a tool to functionalize interfaces, e.g. in the field of protective coatings, microanalysis or molecular electronics [1–5]. Particular attention has been devoted to the structure of thiols on Au(111) [5] as a model system. However, though the adsorption of thiols on Au(111) was studied thoroughly, both experimentally and theoretically, the actual adsorption site of the thiolate adsorbate has remained puzzling for years. While most computational studies favoured a bridge site with the S-atom slightly shifted towards the fcc hollow position [6–11], there are experimental hints that the S-atom occupies a top position [12, 13].

Furthermore, STM experiments could show that both methanethiolate and benzenethiolate are able to induce reconstruction effects on Au surfaces and to form surface structures involving a Au-adatom [14, 15]. While X-ray standing wave and photoemission experiments suggest a model involving one Au adatom per methanethiolate [16, 17], a model consisting of Au-adatom complexes with two methanethiolates is deduced from STM experiments [18]. For larger alkane chain thiolates the adatom model involving one Au adatom per molecule is favoured as well [19]. Various DFT-studies proposed different models of stable reconstructions for thiolate molecules on Au(111) (see, e.g., Ref. [20] for a recent review).

The surface restructuring in response to changes in environmental conditions is of strong current interest, also in the field of heterogeneous catalysis [21]. Furthermore, nanostructured surfaces often exhibit adsorption properties that distinctly different from those of flat surfaces [22–24]. Therefore we have studied the binding of thiolates on flat Au(111) and the adsorption-induced restructuring on the basis of periodic density functional theory calculations. Defect structures are created in a systematic way in order to explain the stability of a distinct model over the other. Furthermore, the impact of the coverage and in an implicit way also the chemical environment on the stability is addressed. The relation between surface structure and adsorption properties has been discussed on the basis of an analysis of the underlying electronic structure, thus making connection to reactivity concepts at surfaces.

All results for thiolate adsorption have been compared with corresponding results for selenolate adsorption which has been studied less frequently [25–28], but which is also of interest as replacing thiolates with selenolates might improve the overall oxidative and thermal stability of SAMs [25, 27].

II. METHODS

Periodic DFT calculations have been performed using the Vienna ab initio simulation package (VASP) [29, 30]. Electron-electron exchange and correlation interactions have been described within the generalized gradient approximation (GGA) by employing the Perdew, Burke and Ernzerhof (PBE) functional [31]. In order to account for electron-ion interactions, the projector augmented wave (PAW) method [32, 33] has been used. The impact of van der Waals interactions in these systems has been studied by calculations that employ the semiempirical dispersion correction scheme D3 of Grimme [34]. Screening effects of the substrate in the dispersion interaction have been

accounted for in the way that only the first layer of metal atoms is included in the calculation of the dispersion energy (further on denoted as PBE-D3-1layer). It could be shown that such a crude approximation works rather well for adsorption energies [35–37]. The electronic one-particle wave functions were expanded in a plane wave basis set up to an energy cut-off of 400 eV. The metal surfaces were modeled by a slab consisting of five atomic layers that were separated by a vacuum region of 20 Å. The geometry of the adsorption complex was optimized by relaxing all atoms of the adsorbate and the metal atoms of two uppermost layers of the surface. The layer spacing of the lower layers were taken from the theoretical lattice parameters (4.171 Å).

The adsorption of chalcogenate radicals at various coverages has been modeled by (3×3), $(3 \times 3\sqrt{3})$rect and $(3 \times \sqrt{3})$rect overlayer structures. For these calculations $4 \times 4 \times 1$, $4 \times 2 \times 1$ and $4 \times 9 \times 1$ Monkhorst-Pack k point meshes, respectively, with a Methfessel-Paxton smearing of 0.1 eV were used for the integration over the first Brillouin zone. Isolated molecules in the gas phase were treated employing a large cell (20 Å × 21 Å × 22 Å), the Γ-point only and a Gaussian smearing of 0.01 eV.

The adsorption energy has been defined as

$$E_{\mathrm{ad}} = (E_{\mathrm{tot}} - (E_{\mathrm{surf}} + mE_{\mathrm{mol}}))/m \qquad (1)$$

where E_{tot}, E_{surf} and E_{mol} are the total energy of the relaxed adsorption complex, the energy of the surface and the energy of the isolated molecule, respectively. The number of molecules within a unit cell is given by m.

In order to compare adsorption energies of surfaces including different numbers of vacancies or adatoms, the energy that has to be paid in order to create n_v vacancies or n_a adatoms has to be accounted for. Regarding kink or bulk atoms as reservoir where adatoms stem from or diffuse to, the formation energy of the defect calculates as

$$E_{\mathrm{defect}} = E_{\mathrm{surf}} - E_{\mathrm{Au(111)}} + (n_v - n_a)E_{\mathrm{Au}}^{\mathrm{bulk}}. \qquad (2)$$

Here, E_{surf} and $E_{\mathrm{Au(111)}}$ denote the energy of the surface containing defects and the energy of the unreconstructed (111) surface, respectively. $E_{\mathrm{Au}}^{\mathrm{bulk}}$ is the cohesive energy of Au, that was calculated to be 3.27 eV. Finally, the net adsorption energy can be calculated:

$$E_{\mathrm{ad}}^{\mathrm{net}} = (mE_{\mathrm{ad}} + E_{\mathrm{defect}})/m. \qquad (3)$$

III. RESULTS AND DISCUSSION

A. Adsorption of methanechalcogenates at the unreconstructed Au(111) surface

As starting point the adsorption of methanechalcogenates on the unreconstructed Au(111) surface has been considered. In order to figure out whether there is a trend within the chalcogens the higher homologous element Te has been included in first studies as well.

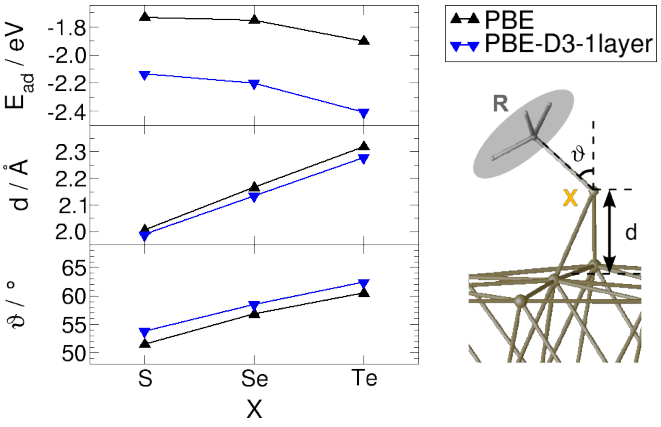

FIG. 1. The impact of different chalcogens on the adsorption properties of isolated methanechalcogenates within a 3 × 3 geometry on Au(111). The adsorption energy E_{ad}, the adsorption distance between the chalcogen atom and the average height of the uppermost Au atoms d and the inclination angle between the chalcogen-carbon bond and the surface normal ϑ are plotted on the left, the parameters are graphically defined on the right.

The adsorption properties of isolated methanethiolate (MeS), methaneselenolate (MeSe) and methanetellurate (MeTe) within a (3×3) overlayer structure on an unreconstructed Au(111) surface are compared in Fig. 1. All methanechalcogenates adsorb preferentially on a bridge position slightly shifted towards the fcc hollow site. This finding agrees well with other theoretical studies regarding the adsorption of thiolates on Au(111) [6–11]

By going from MeS to MeSe and MeTe the adsorption distance (d) and the inclination angle (ϑ) increase. Furthermore, with increasing atomic number of the chalcogen the absolute amount of the adsorption energy increases: whilst MeS yields an adsorption energy of -1.73 eV, the respective values for MeSe and MeTe are -1.75 eV and -1.90 eV. Such a behavior can be rationalized by the increasing size of the orbitals with increasing atomic number of the chalcogen. Thus the equilibrium distance of adsorption gets larger and allows thereby for a stronger inclination of the chalcogen-carbon bond from the surface normal in order to maximize the overlap between the molecule's and the substrate's orbitals. The results of the adsorption properties are in qualitative agreement with a previously published DFT study of the adsorption of MeS and MeSe on Au(111) that used ultrasoft pseudopotentials [38]. Besides, the trend of stronger adsorption with higher atomic number of the chalcogen has also been observed experimentally using high resolution X-ray photoelectron spectroscopy [39].

As far as the inclusion of dispersive interactions is concerned, they only lead to small structural changes in the adsorption complex of methanechalcogenates on

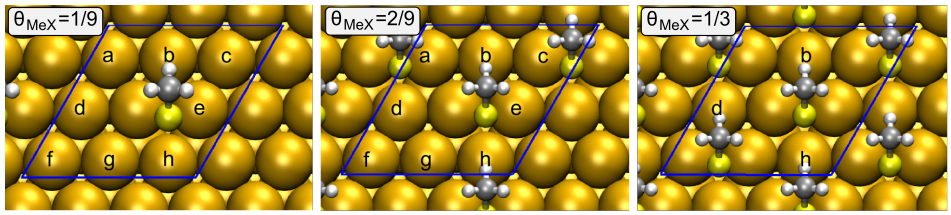

c(defect)	missing atoms	CN
1/9	h	8
2/9	h+b	7
3/9	h+f+g	7
3/9*	h+b+d	6
4/9	h+b+f+g	6
5/9	h+b+f+g+d	5
6/9	h+b+f+g+a+c	5
7/9	h+b+f+g+a+c+d	4
8/9	h+b+f+g+a+c+d+e	3

FIG. 2. Top views of the structures of MeX adsorbed on Au(111) at different coverages (θ_{MeS}). Defect structures are created by subsequently removing the Au atoms a-h of the (3×3) unit cell. The table on the right assigns the defect concentration (c(defect)), that is defined as number of vacancies per surface atom, to the respective structure used in the calculation and to the coordination number (CN) of the Au atoms in the surface that bind to the X-atom of MeX. As two different structures are used for a defect concentration of 1/3, one of them is labeled by a star (*).

Au(111), as shown in Fig. 1. Due to the rather large dispersion coefficient of Au the inclusion of dispersive interactions increases the absolute amount of the adsorption energy significantly (about 0.4 to 0.5 eV). However, the differences in the adsorption energies of MeS, MeSe and MeTe remain nearly constant. Additionally, as methanechalcogenates are rather small molecules, the impact of intermolecular dispersion interactions is supposed to be small as well. Indeed, test studies employing the PBE-D3-1layer method showed, that dispersion interactions between MeS molecules in a $(\sqrt{3} \times \sqrt{3})R30°$ overlayer structure on Au(111) are smaller than 80 meV and thus make up less than 4% of the total adsorption energy. The energetic differences between various structures, which is the main interest in this work, depend even less on dispersion. Thus, we judge the pure PBE functional to be suitable in this case and van der Waals interactions were not included for further studies comparing the adsorption of MeS and MeSe.

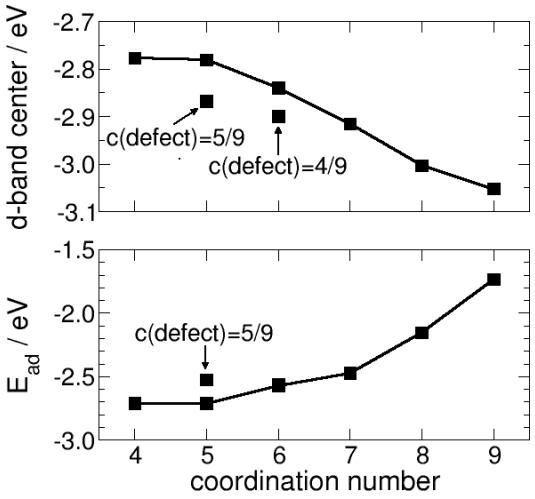

FIG. 3. The correlation between the energetic position of the center of the d-band of the two Au atoms that bind to MeS and the adsorption energy per MeS molecule in different defect structures is shown. Connecting lines are just a guide to the eyes.

B. Systematic construction of defect structures

Using a (3×3) supercell of the Au(111) surface different methanechalcogenate coverages are realized: they employ 1, 2 or 3 MeS molecules per 9 substrate atoms and will consequently be referred to as a MeX coverage (θ_{MeS}) of 1/9, 2/9 or 1/3 further on. For all coverages defect structures are systematically constructed by removing Au-atoms of the (3×3) unit cell as indicated by the graphical scheme shown in Fig. 2.

In all structures involving a defect concentration up to 7/9, the chalcogenate molecule remains at the bridge-fcc adsorption site and only Au atoms in the surroundings are taken off. Obviously, by removing atoms of the surface the coordination number of the Au atoms that bind to the chalcogenate molecule is reduced. As expected according to the d-band model for late transition metals [40] this reduction of the coordination number leads to an increase of both the center of the d-band and the absolute value of the adsorption energy. Figure 3 shows this relation for the adsorption of MeS on Au(111) containing defects.

In the structure with a defect concentration of 8/9 MeX, adsorbs ontop of the adatom (further on also denoted as Au-MeX). In contrast to the previously discussed binding situations, the S-atom only binds to one Au-atom. However as this Au-atom is only three-fold coordinated at the surface it is highly reactive and the energy gain due to that bond formation (E_{ad}=-2.01 eV both for MeS and MeSe) is larger than the energy gain due to the adsorption of MeS or MeSe on the unreconstructed surface (E_{ad}=-1.73 eV for MeS and -1.75 eV for MeSe).

So far, the energetic costs to create the defect have been neglected. However, only by introducing a defect formation energy, e.g. as done in eq. 2, the stability of structures with different numbers of defects can be equitably compared. The resulting net adsorption energies, $E_{\mathrm{ad}}^{\mathrm{net}}$, are plotted relative to $E_{\mathrm{ad}}^{\mathrm{unrecon}}$ as a function of the defect concentration in Fig. 4. Negative values reveal that the adsorbate is able to induce reconstruction

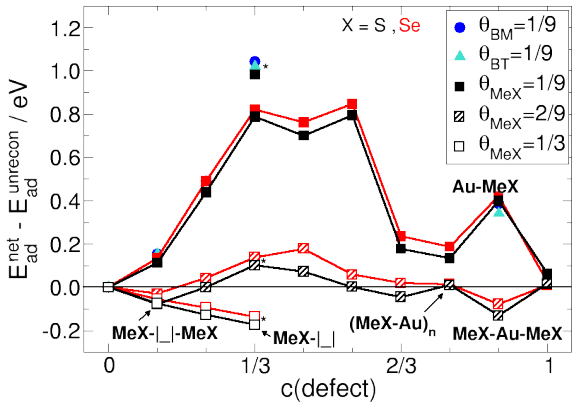

FIG. 4. The net adsorption energy relative to the adsorption energy of the unreconstructed adsorption complex ($E_{\rm ad}^{\rm net} - E_{\rm ad}^{\rm unrecon}$) is shown for different chalcogenate molecules (benzenethiolate (BT), benzylmercaptane (BM), methanethiolate (MeS) and methaneselenolate (MeSe)) and different coverages as a function of the defect concentration (c(defect)). The structures corresponding to certain defect concentrations are constructed as described in Fig. 2. Connecting lines are just a guide to the eyes.

effects. Comparing the two methanechalcogenates MeS and MeSe there is hardly any difference in the net adsorption energies. The stability of all defect structures studied is slightly lower for MeSe compared to MeS. Yet, there are distinct differences regarding the molecular coverage. The values of $E_{\rm ad}^{\rm net}$ for a molecular coverage of 1/9 suggest that a chalcogenate molecule adsorbed on Au(111) without any interaction to neighboring adsorbates is not able to create any reconstruction of the surface. The energetic costs to create the defect within the surface cannot be counterbalanced by the energy gain due to the adsorption at lower coordinated adsorption sites. Consequently, at low coverages also the widely discussed model consisting of a Au-adatom and a single thiolate molecule (Au-MeS) can only be stable if the Au-adatoms are already available at the surface. If the energetic costs to create a Au-adatom are taken into account, the model of a Au-adatom-monothiolate moiety is thermodynamically unstable.

By increasing the coverage of the molecules and keeping the concentration of defects constant, several molecules can share a defect site and profit from the energy gain, while the energetic costs to create the defect stay the same. Such a mechanism enables adsorbate induced reconstruction effects.

The easiest and probably also most prominent model of stable reconstruction effects is indeed given by the adatom-dithiolate model of Maksymovych, in which two thiolate molecules share one Au-adatom (MeX-Au-MeX). Other types of reconstruction that are thermodynamically possible at higher coverages reveal 1:1 and 1:2 ratios of vacancies to molecules, further on denoted as (MeX-␣) and (MeX-␣-MeX), respectively. According to this analysis, the model of polymeric chains of MeS-Au moieties ($(\text{MeX-Au})_n$), introduced by Grönbeck *et al.* [41], seems to be hardly stabilized.

C. Stability of different reconstruction models at different environmental conditions

The structural motifs identified in the (3×3) unit cell are now used for a more detailed study on the impact of the molecular coverage. The considered structures are illustrated in Fig. 5 As shown in Fig. 6, also for other molecular coverages substrate reconstruction is slightly less stable for MeSe compared to MeS, but the trend in the coverage dependent results of the two chalcogenates is the same. The model of an adatom-monochalcogenate moiety (Au-MeX) is significantly less stable than the adsorption at the unreconstructed surface. Although the difference $E_{\rm ad}^{\rm net} - E_{\rm ad}^{\rm unrecon}$ decreases with increasing coverage, adsorption without reconstruction remains about 0.3 eV for MeS and about 0.35 eV for MeSe more favorable. In contrast, polymeric chains ($(\text{MeX-Au})_n$), that exhibit the same adatom-to-molecule ratio as the Au-MeX model, are of comparable stability as the adsorption complex without any reconstruction effects. But also for this model no clear preference of reconstruction effects can be deduced at any coverage. A distinct stabilization both at low coverage (-0.26 eV for MeS, -0.18 eV for MeSe) and at high coverage (-0.20 eV for MeS, -0.14 eV for MeSe) is obtained for a 1:2 ratio of adatoms to molecules (MeX-Au-MeX model).

By looking at the redistribution of the charge density due to MeS adsorption (Fig. 7), these results for different adatom-models can be nicely explained. In the Au-MeS model only one strong covalent bond is formed between the S-atom of the thiolate molecule and the Au adatom. This is indicated both by the enhanced charge density in between the adsorbate and the adatom and by a rather short Au-S-distance of 2.28 Å. In the polymeric chain model, the thiolate's S-atom can establish two covalent bonds to the adjacent adatoms. Although each of the two bonds is slightly weaker and correspondingly somehow longer than the Au-S bond in the Au-MeS model, a stronger total interaction is obtained. However, in both models no direct interaction with the underlying surface occurs. This is also revealed by the rather large distance between the S-atom and the closest Au-atom of the surface (3.54 Å) in the $(\text{MeS-Au})_n$ model. In the MeS-Au-MeS model, both a covalent bond to the adatom and a surface atom is formed. Additionally, as the density of adatoms with respect to the molecular density is only half, less energy has to be paid for creating the adatoms. Thus, this model is the most favorable one at all considered coverages.

Furthermore, structures involving vacancy sites are considered in Fig. 6. The creation of a vacancy site in the surface is only exothermic, if at least two molecules

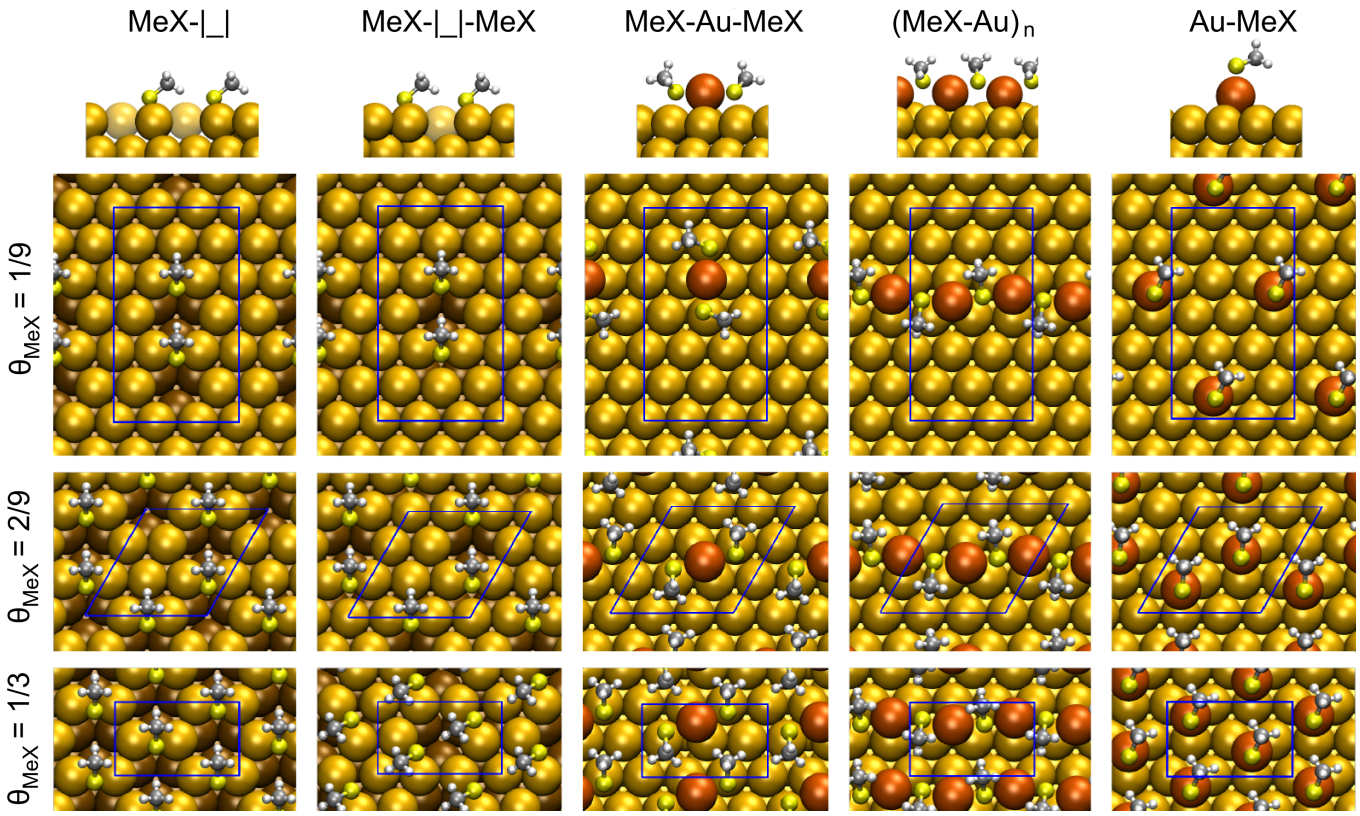

FIG. 5. Side and top views of different reconstruction motifs at different molecular coverages.

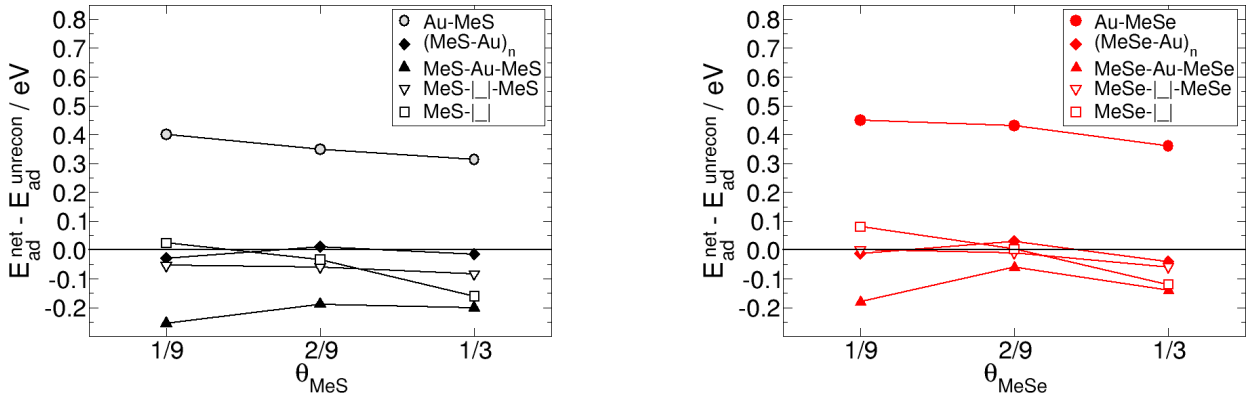

FIG. 6. The net adsorption energy relative to the adsorption energy of the unreconstructed adsorption complex ($E_{\mathrm{ad}}^{\mathrm{net}} - E_{\mathrm{ad}}^{\mathrm{unrecon}}$) is shown for different reconstruction motifs as a function of the MeX coverage. Connecting lines are just a guide to the eyes.

benefit from the increased reactivity in Au atoms surrounding the vacancy. Hence, at a molecular coverage of 1/9, the model with one vacancy site per two thiolate molecules (MeS-⊔-MeS) is thermodynamically stable, in contrast to the model with one vacancy site per thiolate (MeS-⊔). At that coverage the MeS-⊔ model provides only one defect that is shared by two molecules, the other vacancy does not affect more than one adsorbate. Only by doubling the molecular coverage, the second vacancy influences the Au atoms bound to a further molecule and thus $E_{\mathrm{ad}}^{\mathrm{net}} - E_{\mathrm{ad}}^{\mathrm{unrecon}}$ decreases and even gets negative for MeS. Although the trend is the same for MeSe, the relative energies of structures involving vacancies are smaller and neither at a coverage of 1/9 nor at a coverage of 2/9 a distinct stability of reconstruction motifs including vacancies can be observed. In the close-packed structure, however, the higher density of vacancies provided by the MeX-⊔ model as compared to the MeX-⊔-MeX model

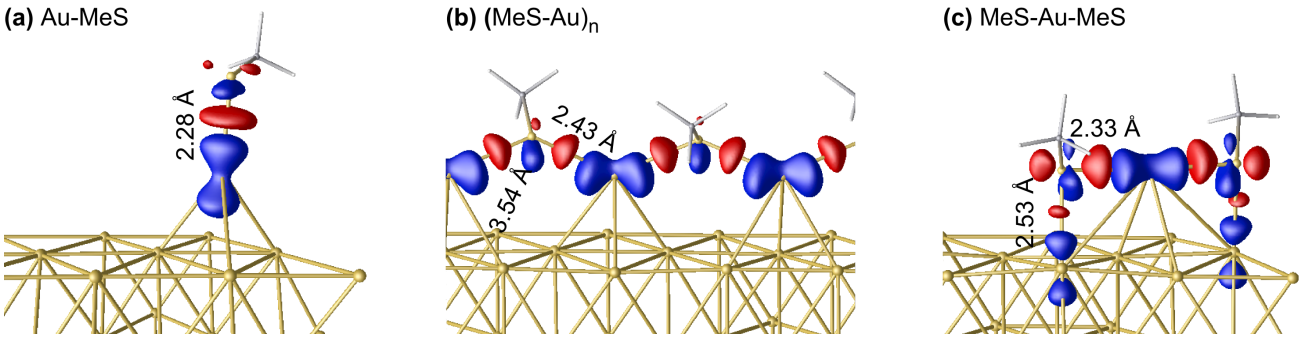

FIG. 7. Isosurfaces at values of +0.05 e/Å^3 (red) and -0.05 e/Å^3 (blue) of the charge density difference of different adatom-models in a (3×3) overlayer structure of MeS on Au(111) are shown. Besides, the distances between the thiolate's S-atom and the closest Au-atoms are indicated.

leads to clearly stabilized structures both for MeS and MeSe. In that structure the two Au atoms bound to the chalcogenate molecule are surrounded by four vacancies and are thus highly reactive. This defect-rich structure corresponds to the honeycomb structure that has already been introduced by Molina and Hammer [42].

Finally, at all coverages the most stable structural motif of reconstruction is given by the adatom-dichalcogenate model (MeX-Au-MeX). Yet, when going to higher coverages methyl groups of neighboring molecules start interacting repulsively and the stability decreases. At saturation coverage (θ_{MeS}=1/3), the MeX-Au-MeX model is only slightly more stable than the MeX-⊔ model ($\Delta E_{\mathrm{ad}}^{\mathrm{net}}$=40 meV for MeS and 20 meV for MeSe). Further test studies of structures with vacancies sites located close to the adatom-dithiolate moiety did not yield more favorable net adsorption energies.

So far, various structures have been studied explicitly as a function of the MeS coverage. Using the ab initio atomistic thermodynamics approach the results can be related to the chemical potential as shown in Refs. [8, 43–47].

However, less attention has been paid to the dependence on the energetics of the Au adatom. Different mechanisms for the creation of the adatoms have been suggested. Partly, they could stem from the lifting of the herringbone reconstruction, they could be created locally or as mentioned already stem from kink sites. The dominating mechanism might again depend on the experimental conditions and depending on the actual mechanism different energies are needed to create the defect. E.g. it has been shown, that the diffusion of adatoms is considerably faster at the solid/liquid surface compared to the solid/vacuum surface, which was not only traced back to smaller activation barriers for the adatom diffusion on the surface but also to an alleviated release of the adatom [48]. In particular if a SAM is formed by immersion into a thiol solution, solvent molecules might stabilize defect structures (E_{surf}) compared to the unreconstructed surface ($E_{\mathrm{Au(111)}}$) which will decrease E_{defect} as defined in equation 2. Furthermore, temperature might facilitate adatom formation.

In the following, using the concept of *ab initio* thermodynamics [49, 50], the relative stability of various structures is studied as a function of the chemical potential of the thiolate molecule, $\Delta\mu_{\mathrm{MeS}}$, and of the energy needed to create the defect, E_{defect}^{+}, whereby + denotes the deviation from the energy needed to create the defect at the solid/vacuum interface as defined in equation 2. E_{defect}^{+} might also be understood as a measure of the defect concentration that is already present prior to adsorption. Neglecting entropic contributions the Gibbs free energy of adsorption per surface unit area is approximated according to:

$$\Delta G_{\mathrm{ad}}(\Delta\mu_{\mathrm{MeX}}, E_{\mathrm{defect}}^{+}) = \frac{1}{A}(mE_{\mathrm{ad}} - m\Delta\mu_{\mathrm{MeX}} - E_{\mathrm{defect}}^{+}) \tag{4}$$

where m denotes the number of molecules within the unit cell and A is the area of the unit cell of the respective structure.

In Fig. 8, the phase diagram of the stable MeS and MeSe adsorption structures shown in Fig. 5 is plotted given by the minimum $\Delta G_{\mathrm{ad}}(\Delta\mu_{\mathrm{MeX}}, E_{\mathrm{defect}}^{+})$ as a function of the relative defect energy E_{defect}^{+} and the chemical potential of MeS and MeSe, respectively. E_{defect}^{+} is given as a fraction/multiple of the value E_{defect} as defined in equation 2. E_{defect} can be seen as reference energy for creating defects in vacuum. However, depending on the experimental conditions defect structures of the substrate could be stabilized or destabilized, i.e. by solvation and temperature effects or applied electric potentials. The 2D intersection of ΔG_{ad} shown in Fig. 8 is chosen to reveal the most stable structures. As expected the results for MeS and MeSe are again very similar. For low chemical potentials of MeX (i.e. low concentrations) the clean Au(111) surface and the adsorbate in gas phase / solution is the most stable state. If the chemical potential is increased and the costs to create defect structures are low, the vacancy rich structure MeX-⊔ with a MeX coverage of 1/3 is realized. For defect energies close to the solid/vacuum value calculated according to

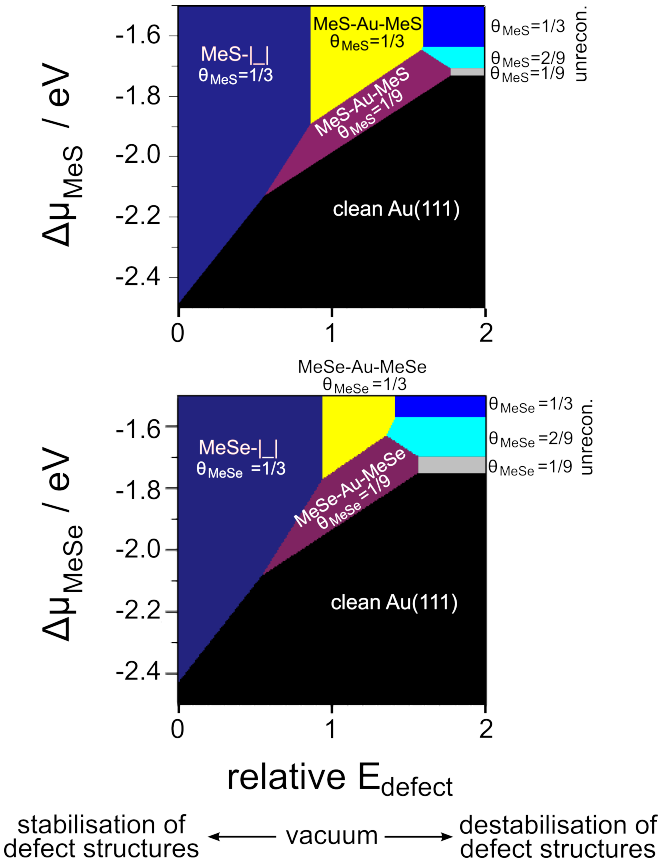

FIG. 8. Most stable structures in dependency of the chemical potential of the MeX radical and the relative energy needed to create the defect structure. A relative defect energy of 0 means that no energy is needed to create the defect, while the value of 1 is chosen to represent the energy needed to create the defect by releasing or shifting atoms from or to kink sites.

equation 2 the adatom-dichalcogenate models MeX-Au-MeX at a coverage of 1/9 and 1/3 are the most stable structures at elevated chemical potentials. At a certain E^{+}_{defect} the costs to create defects are too large to yield stable reconstruction motifs and adsorption at the unreconstructed surface is obtained by increasing the chemical potential of MeX. Comparing the plots for MeS and MeSe in detail some differences can be spotted. In case of MeSe, the slightly lower stability of adsorption structures including reconstructions of the substrate leads in Fig. 8 to a larger region of stability of unreconstructed adsorption structures and a less extended region of stability for the MeSe-Au-MeSe model. Besides the stability region of the MeS-⊔ reconstruction motif at a molecular coverage of 1/3 is extended to higher defect energies.

These qualitative considerations about the stability of defect structures are to be seen as a first approximation. They imply that different defect structures are (de)stabilized to the same extend, which might not be true. Therefore, it would be very interesting to study e.g. the impact of solvent molecules on the stability of different defect structures explicitly.

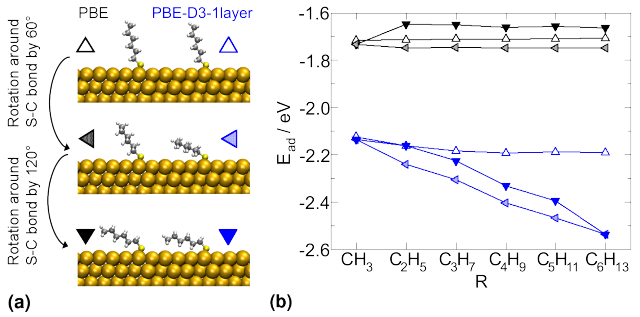

FIG. 9. (a) Different (meta-)stable configurations of hexanethiolate adsorbed on Au(111) obtained by the pure PBE functional and PBE-D3-1layer method. In (b) the respective adsorption energies of alkanethiolates of different chain lengths (S-R) are shown.

Furthermore, the actual experimentally observed structures might be more complicated implying larger unit cells in which different reconstruction models could be realized and coexist. However, this is somehow beyond the scope of this study, as it only intends to show trends of different structural motifs at different coverages using rather simple models.

D. Transferability to SAMs composed of chalcogenates with larger rest groups

Finally the question arises whether this comparison of the adsorption of MeS and MeSe on Au(111) could also be an adequate model for the adsorption of chalcogenates involving larger rest groups R.

Therefore the adsorption of a homologous series of alkanethiolates on Au(111) has been calculated. As shown in Figure 9 pure PBE calculations suggest for all alkanethiolates studied the tilted configuration to be the most stable one. The experimentally observed and thus expected flatly lying configuration is calculated to be the least stable one, although the energetic differences between the different configurations are small. Furthermore, PBE hardly discriminates between alkanethiolates with different chain lengths. They are all supposed to have almost the same adsorption energy. Including van der Waals interactions via the PBE-D3-1layer method, there is a difference between upright standing, tilted and flatly lying alkanethiolate molecules. For upright standing alkanethiolates van der Waals interactions mainly shift the total adsorption energy but there is also almost no energy gain by going to longer alkyl chains, i.e. dispersion interactions between the substrate and upright standing alkyl groups, as present in close-packed SAMs, are negligible. Furthermore, the changes in the local adsorption geometry of the head group are small if the upright standing chain length is increased: the adsorption

distance does not vary by more than 3% and the inclination angle bends by less than 18%. Thus, for studying the nature of reconstruction effects due to the adsorption of thiolates on Au(111) in close-packed structures the simplest alkanethiolate, methanethiolate (MeS), is a suitable representative, since the rest groups of alkanethiolate molecules hardly influence the chemical bond between the head group and the surface.

This assumption was verified and indeed extended to aromatic rest groups by using benzylmercaptane (BM) and benzenethiol (BT) molecules to recalculate some of the models of the systematic study of reconstruction effects as well. Figure 4 shows that they indeed follow the same trend and actually lead to almost the same net adsorption energies as MeS.

However, these systems are somehow artificial and should rather be seen as a model for the S-Au interaction in close packed BM and BT SAMs, since van der Waals interactions were not included in this study. At such a low coverage, BT and BM would adsorb flatly on Au, if van der Waals interactions were accounted for. This is also shown in Fig. 9 for the adsorption of alkanethiolates on Au(111) at low coverages: van der Waals interactions are indispensable to correctly describe the most stable configuration, i.e. the flatly lying configuration. Only by including dispersion interactions the trend of increasing the adsorption energy by increasing the rest group can be reproduced.

IV. CONCLUSIONS

Using periodic density functional theory calculations, we have addressed the adsorption of methanethiolate (MeS) and methaneselenolate (MeSe) on Au(111) including defect structures. The adsorption properties of MeS and MeSe on Au(111) are very similar. Both are able to induce substrate reconstructions, although reconstruction effects are slightly less stable for selenium compounds. Substrate reconstruction is yet only possible if at least two molecules can benefit from the energetic gain due to the adsorption at the defect site. Regarding the adsorption at the solid/vacuum interface the adatom-dichalcogenate model of Maksymovych is the most stable reconstruction motif for various coverages. However if defect structures are somehow stabilized (e.g. by solvent, temperature or electric potentials) the honeycomb structure of Molina and Hammer is found to be the most stable structure among the structures studied herein. Only if defect structures are destabilized adsorption at the unreconstructed surface should occur in thermodynamic equilibrium. Finally, to some extent, the adsorption of MeS and MeSe can serve as models for the adsorption of larger chalcogenate molecules.

ACKNOWLEDGEMENT

Computer time has been provided by the BW-Grid and the BW-Uni-Cluster projects of the federal state of Baden-Württemberg.

[1] A. Ulman, Chem. Rev. **96** (1996) 1533.
[2] F. Schreiber, Prog. Surf. Sci. **65** (2000) 151 .
[3] J. C. Love, L. A. Estroff, J. K. Kriebel, R. G. Nuzzo, and G. M. Whitesides, Chem. Rev. **105** (2005) 1103.
[4] H.-G. Boyen, P. Ziemann, U. Wiedwald, V. Ivanova, D. M. Kolb, S. Sakong, A. Groß, A. Romanyuk, M. Büttner, and P. Oelhafen, Nature Mater. **5** (2006) 394.
[5] M. Kind and C. Wöll, Prog. Surf. Sci. **84** (2009) 230.
[6] J. Nara, S. Higai, Y. Morikawa, and T. Ohno, J. Chem. Phys. **120** (2004) 6705.
[7] A. Bilić, J. R. Reimers, and N. S. Hush, J. Chem. Phys. **122** (2005) 094708.
[8] J. Kučera and A. Groß, Langmuir **24** (2008) 13985.
[9] J. Kučera and A. Groß, Phys. Chem. Chem. Phys. **12** (2010) 4423.
[10] X. Stammer, K. Tonigold, A. Bashir, D. Käfer, O. Shekhah, C. Hülsbusch, M. Kind, A. Groß, and C. Wöll, Phys. Chem. Chem. Phys. **12** (2010) 6445.
[11] K. Forster-Tonigold, X. Stammer, C. Wöll, and A. Groß, Phys. Rev. Lett. **111** (2013) 086102.
[12] M. Roper, M. Skegg, C. Fisher, J. Lee, V. Dhanak, D. Woodruff, and R. G. Jones, Chem. Phys. Lett. **389** (2004) 87 .
[13] H. Kondoh, M. Iwasaki, T. Shimada, K. Amemiya, T. Yokoyama, T. Ohta, M. Shimomura, and S. Kono, Phys. Rev. Lett. **90** (2003) 066102.
[14] P. Maksymovych, D. C. Sorescu, and J. T. Yates, Phys. Rev. Lett. **97** (2006) 146103.
[15] P. Maksymovych and J. T. Yates, J. Am. Chem. Soc. **130** (2008) 7518.
[16] M. Yu, N. Bovet, C. J. Satterley, S. Bengió, K. R. J. Lovelock, P. K. Milligan, R. G. Jones, D. P. Woodruff, and V. Dhanak, Phys. Rev. Lett. **97** (2006) 166102.
[17] A. Chaudhuri, T. Lerotholi, D. Jackson, D. Woodruff, and V. Dhanak, Surf. Sci. **604** (2010) 227.
[18] O. Voznyy, J. J. Dubowski, J. T. Yates, and P. Maksymovych, J. Am. Chem. Soc. **131** (2009) 12989, PMID: 19737018.
[19] F. Li, L. Tang, W. Zhou, and Q. Guo, J. Am. Chem. Soc. **132** (2010) 13059.
[20] H. Häkkinen, Nature Chem. **4** (2012) 443.

[21] F. Tao, M. E. Grass, Y. Zhang, D. R. Butcher, F. Aksoy, S. Aloni, V. Altoe, S. Alayoglu, J. R. Renzas, C.-K. Tsung, Z. Zhu, Z. Liu, M. Salmeron, and G. A. Somorjai, J. Am. Chem. Soc. **132** (2010) 8697.

[22] A. Groß, J. Comput. Theor. Nanosci. **5** (2008) 894.

[23] T. Waldmann, C. Nenon, K. Tonigold, H. E. Hoster, A. Groß, and R. J. Behm, Phys. Chem. Chem. Phys. **14** (2012) 10726.

[24] H. Hu, L. Reven, and A. D. Rey, Molecular Simulation **39** (2013) 292.

[25] F. K. Huang, R. C. Horton, D. C. Myles, and R. L. Garrell, Langmuir **14** (1998) 4802.

[26] J. K. Lim and S.-W. Joo, Appl. Surf. Sci. **253** (2007) 4830 .

[27] J. N. Hohman, J. C. Thomas, Y. Zhao, H. Auluck, M. Kim, W. Vijselaar, S. Kommeren, A. Terfort, and P. S. Weiss, J. Am. Chem. Soc. **136** (2014) 8110.

[28] F. P. Cometto, C. A. Caldern, M. Morn, G. Ruano, H. Ascolani, G. Zampieri, P. Paredes-Olivera, and E. M. Patrito, Langmuir **30** (2014) 3754, PMID: 24645647.

[29] G. Kresse and J. Furthmüller, Phys. Rev. B **54** (1996) 11169.

[30] G. Kresse and J. Furthmüller, Comput. Mater. Sci. **6** (1996) 15.

[31] J. P. Perdew, K. Burke, and M. Ernzerhof, Phys. Rev. Lett. **77** (1996) 3865.

[32] P. E. Blöchl, Phys. Rev. B **50** (1994) 17953.

[33] G. Kresse and D. Joubert, Phys. Rev. B **59** (1999) 1758.

[34] S. Grimme, J. Antony, S. Ehrlich, and H. Krieg, J. Chem. Phys. **132** (2010) 154104.

[35] G. Mercurio, E. R. McNellis, I. Martin, S. Hagen, F. Leyssner, S. Soubatch, J. Meyer, M. Wolf, P. Tegeder, F. S. Tautz, and K. Reuter, Phys. Rev. Lett. **104** (2010) 036102.

[36] K. Tonigold and A. Groß, J. Comput. Chem. **33** (2012) 695.

[37] F. Buchner, K. Forster-Tonigold, B. Uhl, D. Alwast, N. Wagner, H. Farkhondeh, A. Groß, and R. J. Behm, ACS Nano **7** (2013) 7773.

[38] E. de la Llave and D. A. Scherlis, Langmuir **26** (2010) 173.

[39] T. Weidner, A. Shaporenko, J. Müller, M. Höltig, A. Terfort, and M. Zharnikov, J. Phys. Chem. C **111** (2007) 11627.

[40] B. Hammer and J. Nørskov, Adv. in Catal. **45** (2000) 71.

[41] H. Grönbeck and H. Häkkinen, J. Phys. Chem. B **111** (2007) 3325.

[42] L. M. Molina and B. Hammer, Chem. Phys. Lett. **360** (2002) 264.

[43] P. Carro, R. Salvarezza, D. Torres, and F. Illas, J. Phys. Chem. C **112** (2008) 19121.

[44] P. Carro, D. Torres, R. Diaz, R. C. Salvarezza, and F. Illas, J. Phys. Chem. Lett. **3** (2012) 2159.

[45] P. Carro, X. Torrelles, and R. C. Salvarezza, Phys. Chem. Chem. Phys. **16** (2014) 19017.

[46] C. Vericat, M. E. Vela, G. Benitez, P. Carro, and R. C. Salvarezza, Chem. Soc. Rev. **39** (2010) 1805.

[47] E. Pensa, E. Corts, G. Corthey, P. Carro, C. Vericat, M. H. Fonticelli, G. Bentez, A. A. Rubert, and R. C. Salvarezza, Acc. Chem. Res. **45** (2012) 1183.

[48] J. M. Dona and J. Gonzalez-Velasco, J. Phys. Chem. **97** (1993) 4714.

[49] K. Reuter and M. Scheffler, Phys. Rev. B **65** (2001) 035406.

[50] F. Gossenberger, T. Roman, and A. Groß, Surf. Sci. **631** (2015) 17.